

UAS Propeller/Rotor Sound Pressure Level Reduction Through Leading Edge Modification

Callender MN*

Middle Tennessee State University, USA

Abstract

Manned aviation is regulated by the Federal Aviation Administration (FAA) to provide for safe, secure, efficient, and environmentally responsible aviation in the United States. One environmental issue regulated by the FAA is the noise created by aircraft. Federal Aviation Regulation (FAR) Title 14 Part 36 deals specifically with sound pressure levels (SPL) per aircraft type when the aircraft are in close proximity to the ground. Minimizing aircraft noise helps to maintain positive relationships between the aviation community and the general public. Unmanned aircraft systems (UAS) are a very rapidly growing segment of the aviation industry that operate within the National Airspace System (NAS); however, there is currently no regulation for UAS SPL. The UAS are regulated, as of August 29, 2016, such that they are mandated to be in close proximity to the ground (no higher than 400 ft). As with manned aircraft, UAS produce high levels of SPL, much of which is due to the propellers/rotors. The combination of proximity to the ground, high SPL, and increasing UAS density will most certainly result in a negative public reaction. To minimize the audible impact of UAS, the author sought to minimize the SPL of small UAS propellers/rotors via leading edge modifications. The modification consisting of a leading edge comb was inspired by one of the three characteristics found on the flight feathers of certain owls: leading edge comb, trailing edge tuft, and upper surface porosity. The modifications could successfully reduce SPL while maintaining constant levels of thrust over a wide range of rpm.

Keywords: Rotor; Pressure

Introduction

The unmanned aircraft systems (UAS) industry is experiencing rapid growth in the military and civilian markets. Technological innovations have progressed to the point where UAS platforms and the sensors that they carry are readily accessible by commercial entities and individuals alike. The rate of proliferation of the systems has outpaced the Federal Aviation Administration's (FAA) ability to codify regulations specific to these aircraft. Several years of regulatory ambiguity coinciding with operation within certificates of authorization (COA) were followed by Section 333 exemptions (3,136 nationally at the time of this writing), operator registration, and now operation under Federal Aviation Regulation (FAR) Title 14 Part 107, Operation and Certification of Small Unmanned Aircraft Systems (sUAS) [1,2]. This new Part of the FARs became effective August 29, 2016. Previously existing Parts of the FARs govern the noise associated with manned aviation. Aircraft certification, aircraft operations, and airport planning as they relate to aircraft noise are regulated by FAR Parts 36, 93, and 150 [3]. These regulations were implemented in the spirit of environmental responsibility. Noise as measured by sound pressure level (SPL) is regulated by the FARs to have minimum impact on the communities and businesses that surround airports within the United States. Prior to the recent effective date for Part 107, the SPL produced by UAS were not regulated by the existing FARs governing manned aviation. Upon inspection of FAR 107, it is clear that the FAA chose not to regulate the SPL of UAS; therefore, UAS will remain outside of noise regulation for the near future. Manned aviation has the greatest perceived SPL when the aircraft are in close proximity to the ground. According to Part 107, UAS are required to remain no higher than 400 ft above ground level (AGL). The exception to this height restriction is if the UAS is being operated near a structure. The aircraft must then remain no more than 400 ft from the structure. The regulation creates the situation where UAS are highly concentrated near the ground. This will bring UAS into closer proximity to communities and businesses. As UAS numbers continue to increase, the noise created by these aircraft may become an area of concern. As with manned aviation, much of the noise created

by unmanned aircraft comes from propellers and/or rotors. Reducing propeller/rotor noise is an active area of research. Results presented by Wisniewski, Byerley, Heiser, Van Treuren, Liller, and Wisniewski showed that sound pressure levels produced by small propellers were reduced by reducing rotational speed and by maximizing nS_bC_L [4]. In this term, n represents the number of blades, S_b represents the area of a blade, and C_L represents a blade's lift coefficient. Wisniewski, Byerley, Heiser, Van Treuren, and Liller developed a computer program to aid in the design of low noise propellers [5]. Wisniewski, Byerley, Heiser, Van Treuren, and Liller minimized the sound produced by a small propeller by using a large number of blades, the GM15 blade section, and an oval tip planform [6]. Lyu, Azarpeyvan, and Sinayoko have numerically predicted that serrations incorporated into the trailing edges of propeller blades would reduce SPL by as much as 7dB [7]. Clark, Alexander, Devenport, Glegg, Jaworski, Daly, and Peake modified the upper surface of wind tunnel models in order to reduce their noise signatures [8]. The upper surface treatment mimicked the upper surface characteristic of the flight feathers of certain owls and produced a reported 10dB reduction in SPL. Callender and Robinson observed noise reductions for propellers with leading edge modifications [9].

The flight feathers of certain owls, to include the Great Grey and the Barn owl, exhibit characteristics like none other in nature. These birds possess comb-like serrations on the leading edge of their flight feathers, a porous or hairy upper surface on the feathers, and a downy

*Corresponding author: Callender MN, Assistant Professor, Middle Tennessee State University, USA, Tel: (615) 598-6552; E-mail: Nate.Callender@mtsu.edu

Received January 18, 2017; Accepted February 20, 2017; Published February 24, 2017

Citation: Callender MN (2017) UAS Propeller/Rotor Sound Pressure Level Reduction Through Leading Edge Modification. J Appl Mech Eng 6: 254. doi: 10.4172/2168-9873.1000254

Copyright: © 2017 Callender MN. This is an open-access article distributed under the terms of the Creative Commons Attribution License, which permits unrestricted use, distribution, and reproduction in any medium, provided the original author and source are credited.



Figure 1: Leading edge serrations and upper surface hairs of owl flight feathers [8,9].

tufted feather trailing edge. The first two owl feather characteristics are shown in Figure 1.

These owls are among the quietest fliers found in nature. Possession of these three unique characteristics and the birds' ability to fly with extremely low noise signatures led researchers to investigate the connection between the two. The work by Clark, et al., Callender and Robinson were focused on one or more of the owls' feather characteristics [8,9].

The motivation for this research was provided by owls' capability to fly silently, thereby having little impact on their surroundings and allowing them to hunt more effectively. The missions of small UAS (sUAS) are different from that of owls; however, noisy flight could prove detrimental through negative public perception. The ability for sUAS to operate in close proximity to the public may be determined by their ability to go unnoticed. The goal of this research is to incorporate biological systems for noise attenuation into sUAS propellers and rotors. Owl feathers operate at very low Re . Propellers and rotors, even those of sUAS, operate at much higher Re . This research evaluated the transferability of a low Re SPL reduction characteristic of owls' feathers into the higher Re regime of sUAS propellers and rotors.



Figure 2: Propeller modifications with leading edge comb tip- and hub-oriented.

Test Equipment

Propulsion system

The propulsion system was comprised of an electric motor and propeller combination appropriate to an sUAS. The motor was a T-Motor MT2212 rated at 980 KV [10]. Two methods of motor control were used. The first method was with an Exceed RC 6-channel digital proportional radio controller. This controller communicated with an Exceed RC FS-R6B 6-channel digital receiver connected to an eRC 25A BEC brushless electric speed controller (ESC) connected to the motor. The second method of control replaced the receiver and radio controller with a solid state circuit and laptop computer. The second method is discussed in the Thrust Stand section. A Turnigy 3,000 mAh 3s 10C lithium polymer (Li-Po) battery pack provided power to the motor. Plastic 8 × 4.5 reverse direction (clockwise), two bladed, fixed-pitch propellers were tested. One propeller was unmodified and provided baseline data. Additional propellers were modified with a leading edge treatment intended to represent a leading edge comb inspired by the leading edge of owls' flight feathers. The leading edge comb was created by hand by carving the leading edge of the propeller blades. One modified propeller was carved such that the comb was oriented toward the propeller blade tips, and the other modified propeller was carved with the comb oriented toward the propeller hub as shown in Figure 2.

Based upon the performance advantage of the hub-oriented comb over the tip-oriented comb, the hub-oriented comb is discussed hereafter.

Sound chamber

For SPL measurements an Extech Instruments USB Sound Level Datalogger was used. The datalogger is shown in Figure 3.

The Extech USB Datalogger offers a range of 30dB to 130dB, ±1.4dB accuracy, A and C weighting, and variable sampling rate using a 0.5 in. shielded electret microphone. The datalogger was placed in a semi-anechoic chamber. The sound chamber consisted of a 36" × 23.5" × 17" wooden box with a removable lid. The sound chamber is shown in Figure 4.

In order to insulate the microphone from external noise and to



Figure 3: Extech Instruments USB Sound Level Datalogger with stand and windscreen used for SPL measurements.



Figure 4: Sound chamber with electric motor, propeller, and sound datalogger installed.

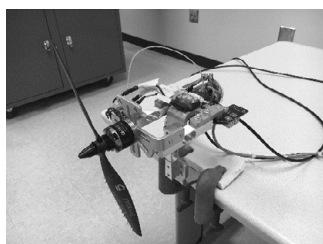


Figure 5: RC benchmark Series 1580 thrust stand and dynamometer with propulsion system installed.

minimize reflection from inside the chamber itself, the inner walls of the sound chamber were covered with egg-crate foam padding. The rim, upon which the lid was placed, was covered with sound absorbing foam. The electric motor and propeller were mounted on a wooden cylindrical post connected to one side of the box, which was itself supported by another cylindrical wooden post connected to the floor of the sound chamber. The motor mounting post was wrapped in sound absorbing foam. The electric motor was connected to the ESC, receiver, and battery, which were placed behind the post connected to the sound chamber's floor. The datalogger was mounted on one of several locations on the sound chamber's floor. The datalogger's cable was ported through a hole in the bottom corner of the sound chamber and was connected via USB to a personal computer (PC) running the Extech Datalogger software. Propeller RPM was measured using an AGPtek Professional Digital Laser Photo Non-Contact Tachometer and reflective tape. The tachometer had a range of 2.5-99,999 RPM, 0.1 RPM resolution, and $\pm 0.05\%$ accuracy.

Thrust stand

A digital thrust stand was used to collect thrust and RPM data and to control the electric motor. The RCbenchmark Series 1580 thrust stand and dynamometer is shown in Figure 5.

The Series 1580 had a vertically-oriented stress member with a Wheatstone bridge strain gage for measuring thrust and two horizontally-oriented stress members with Wheatstone bridge strain

gages for measuring torque. An onboard data acquisition card received the strain gage signals in addition to an RPM signal from the motor. The data acquisition card passed commands from a USB-connected laptop computer to the ESC for motor control. The data acquisition card also monitored the current draw and voltage provided by the battery. The system was capable of measuring thrust to ± 5 kg and torque to ± 1.5 Nm (both with a 0.5% tolerance) and RPM to $\sim 13,000$ RPM (given a 14 pole motor). The Series 1580 allowed propeller thrust and motor efficiency to be measured rapidly and saved as a CSV file that was viewed and manipulated in Microsoft Excel.

Method

Sound testing

SPL testing was conducted by mounting a propeller to the motor inside of the sound chamber. A small piece of reflective tape was adhered to the back face of the propeller in order to measure and set the RPM. The motor was activated by the radio controller, and the RPM was allowed to stabilize. The sound chamber's lid was then installed, and the datalogger was activated. After collecting data at a given RPM, the lid was removed, the RPM was increased via the radio controller and measured by the tachometer. The lid was again replaced and the datalogger again was activated. This procedure was repeated for several RPMs for a given propeller, after which the next propeller was attached, and the tests were repeated.

Thrust testing

The digital thrust stand was first calibrated using a calibration weight and an internal calibration scheme without the propulsion system installed. The motor, ESC, and battery were then installed on the digital thrust stand. A propeller was then installed on the motor. The digital thrust stand was USB connected to a laptop running the RC benchmark software. The software initiated contact with the digital thrust stand, a working directory was chosen, in which the data files were stored, and the load cells were zeroed. The motor's RPM was set by a slider on the software and was allowed to stabilize for at least 5 s. The motor's speed was increased in increments of 200-500 RPM and was allowed to stabilize at each RPM. The RPM slider was brought to zero, a new propeller was installed, and the process was repeated for each propeller. Data was collected continuously throughout each propeller's run.

Results

Raw thrust data collected by the RC Benchmark thrust stand was transferred from the RC Benchmark software to Excel where it was plotted. Curve fitting was performed as is shown for the unmodified propeller in Figure 6.

After curves were fit to each set of data, the thrust curves for each propeller, unmodified and hub-oriented, were compared. The thrust curves for each propeller are presented in Figure 7.

As can be seen in the figure, the leading edge comb modification decreased the amount of thrust produced throughout the RPM range tested. The modified propeller produced approximately 10% less thrust over a majority of the RPM range tested. SPL data for the unmodified and hub-oriented propellers were also curve fitted and shown in Figure 8.

While the leading edge modification resulted in diminished thrust capability, it also decreased the noise signature of the propeller. The SPL reduction was highest at low RPM and decreased as the RPM was increased. The SPL reduction came at the expense of decreased thrust.

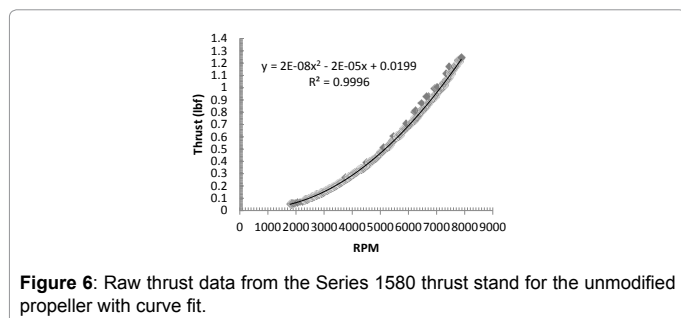


Figure 6: Raw thrust data from the Series 1580 thrust stand for the unmodified propeller with curve fit.

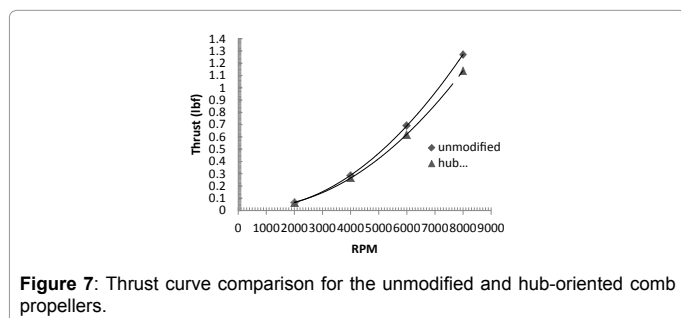


Figure 7: Thrust curve comparison for the unmodified and hub-oriented comb propellers.

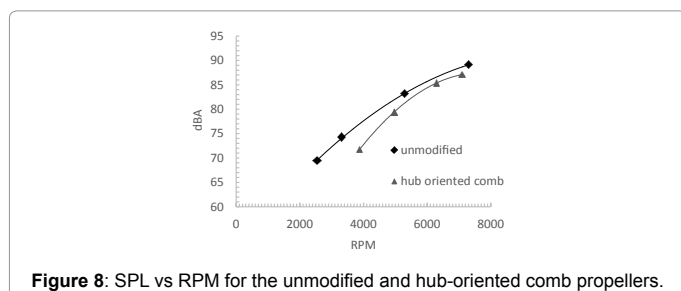
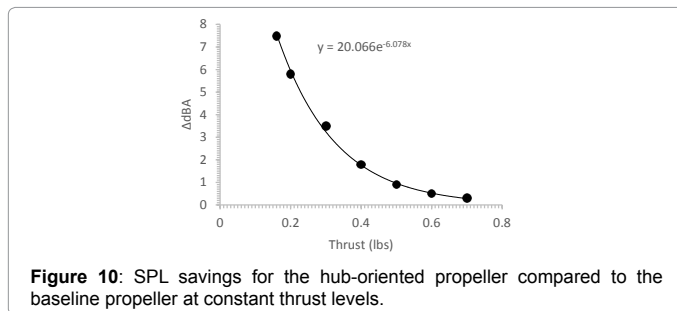
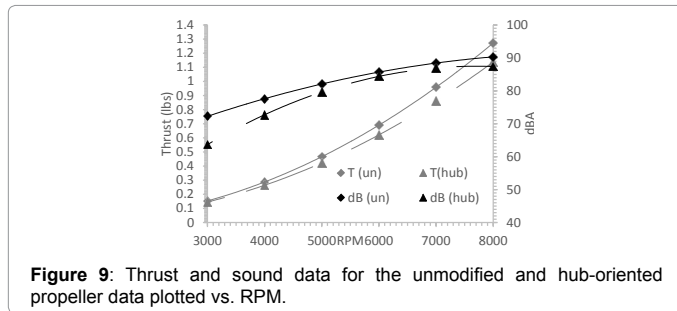


Figure 8: SPL vs RPM for the unmodified and hub-oriented comb propellers.



In order to determine the effectiveness of the propeller modification, the sound reduction was evaluated for constant thrust values. To visualize this, the thrust and SPL plots were combined for ease of comparison as shown in Figure 9.

Lines of constant thrust were drawn from left to right across Figure 8 until points of intersection on the thrust curves were identified. Vertical lines were then drawn from the intersections on the thrust curves to each propeller's *dBA* curve. From these intersections, arrows were drawn to the *dBA* axis on the right. An example of this process is indicated on Figure 8 for a thrust value of 0.3 *lbs*. At this thrust level, the propeller with the hub-oriented leading edge comb required an additional 170RPM to create the same thrust as the unmodified propeller. Increased rotational speed results in a higher noise signature for a given propeller; however, the modified propeller experienced approximately 3.5 *dBA* SPL reduction when compared to the unmodified propeller even while operating at higher RPM. This process was repeated for several thrust values, and the results were plotted and presented in Figure 10.

The figure shows the exponential relationship between the SPL reduction provided by the hub-oriented comb on the leading edge of the modified propeller and the thrust being produced as compared to the unmodified propeller. At high thrust values, in the upper RPM range of the propellers, there is little difference in the SPL values of the modified and unmodified propellers. As thrust decreased, so too did the SPL of each propeller; however, the SPL of the modified propeller decreased at a greater rate than that of the unmodified propeller.

Conclusion

The leading edge modifications inspired by the leading edge comb found on the flight feathers of specific owls was incorporated into a small (8 in. diameter) propeller and was compared to an unmodified propeller. As was expected, both propellers created more thrust and higher SPL as RPM was increased. The propeller with the modified leading edge created less thrust and less SPL than the modified propeller throughout the RPM range tested. This means that the modified propeller had to be operated at higher RPM values in order to produce equivalent thrust values to that of the unmodified propeller. Even when operated at higher RPM (to achieve equivalent thrust), the modified propeller was quieter than the unmodified propeller. The difference in sound grew exponentially as the thrust demand was decreased. Therefore, the hub-oriented leading edge comb was shown to be effective at decreasing the sound produced by small propellers. The increase in the effectiveness of the leading edge comb at lower RPM works to amplify the sound reduction automatically obtained by operating propellers at lower RPM. sUAS operating at low thrust settings would emit lower noise signatures when using propellers with the leading edge comb. Future research efforts will further explore the benefits of using the leading edge comb in addition to combing the other owl feather characteristics in order to minimize the SPL of sUAS propellers and rotors.

References

1. UAS (2016) Commercial UAS exemptions. Association of unmanned Vehicle Systems International.
2. Federal Register (2016) Operation and certification of small unmanned systems.
3. US Government Publishing Office (2016) Electronic code of federal regulations.
4. Wisniewski CF, Byerley AR, Heiser WH, Liller WR (2015) Experimental evaluation of open propeller aerodynamics performance and aero-acoustic behavior. Proceedings of 33rd AIAA Applied Aerodynamics Conference. Dallas American Institute of Aeronautics and Astronautics Inc.
5. Wisniewski CF, Byerley AR, Heiser WH, Liller WR (2015) Designing small propellers for optimum efficiency and low noise footprint. Proceedings of the 33rd AIAA Applied Aerodynamics Conference Dallas.
6. Wisniewski CF, Byerley AR, Heiser WH, Liller WR (2015) The influence of airfoil shape, tip geometry, reynolds number and chord length on small propeller performance and noise. Proceedings of 33rd AIAA Applied Aerodynamics Conference Dallas.
7. Lyu B, Azarpeyvand M, Sinayoko S (2015) A trailing-edge noise model for serrated edges. Proceedings 21st AIAA/CEAS Aeroacoustics Conference Dallas.
8. Clark IA, Alexander WN, Devenport W, Glegg S, Jaworski JW (2015) Bio-inspired trailing edge noise control. Proceedings of the 21st AIAA/CEAS Aeroacoustics Conference Dallas.
9. Callender MN, Robinson V (2016) Small UAS propeller/rotor sound pressure level and thrust testing: bioinspired modifications for UAS noise reduction. Proceedings of Xponential 2016. New Orleans Association of Unmanned Vehicle Systems International.
10. RC Tiger Motor (2016) Professional series motors.